TO THE QUESTION ABOUT THE MECHANISM OF LOW-FREQUENCY MODULATION OF A HIGH-CURRENT RELATIVISTIC ELECTRON BEAM

P. I. MARKOV, I. N. ONISHCHENKO, G. V. SOTNIKOV

National Scientific Center "Kharkiv Institute of Physics and Technology"
(1, Akademichna Str., Kharkiv 61108, Ukraine)

UDC 621.384.6

The results of researches of the propagation of a relativistic electron beam (REB) with a current above the limiting one in a cylindrical drift chamber in the presence of an ion stream are given. The theoretical analysis of the dynamics of electron-ion formation is based on the particle-in-cell (PIC) method. It is shown that the joint injection of a supercritical REB and a low-energy low-current ion beam into the drift chamber can lead to the formation of both the electron virtual cathode and the ion virtual anode. The virtual anode periodically pulses with a low frequency determined by ion motion. The numerical results obtained for hydrogen and nitrogen ions show that the ratio of the frequencies of pulsations is in inverse proportion to the ratio of ion masses. Pulsations of the virtual anode result in a temporal modulation of the electron and ion currents observed at the drift chamber output.

Introduction

The basis of the method of collective acceleration of ions is the slow wave of a space charge formed by a high-current REB as a result of its spatio-temporal modulation. The spatial modulation can be obtained during the propagation of an electron beam through a corrugated metal tube [1] or a drift chamber with the periodic magnetic field created by the system of aluminum and iron rings placed in an outer magnetic field [2]. The necessary temporal modulation can be carried out by a low-frequency variation of the REB current at the input [1, 3, 4].

The low-frequency modulation necessary for ion acceleration can be obtained by passing the high-current electron beam with a current higher than the limiting vacuum one under plasma assistance. In [5], the possible physical mechanism of such a modulation has been suggested. Its idea consists in the following. Let's consider a thin annular electron beam injected into a vacuum cylindrical drift chamber. The space charge limiting current of an electron beam which can propagate through such a system is determined by the expression [6]

$$I_{ce} = \frac{mc^3}{e} \frac{\left(\gamma_e^{2/3} - 1\right)^{3/2}}{2\ln\left(R/r_e\right)}, \qquad (1)$$

where e is the electron charge, m is the electron mass, γ_e is the relativistic factor of an electron beam, R is the radius of the drift chamber, r_e is the radius of an electron beam.

Exceeding the REB current above the limiting value I_{ce} results in the formation of the virtual cathode (VC) reflecting the electrons of a beam. As a result, the electron current lesser than the limiting one propagates behind the virtual cathode area [7]. The reflected particles form a cloud whose parameters (density, location) periodically oscillate in time. The oscillation frequency is proportional to the current of an injected beam [8—10]. These oscillations, in turn, lead to the modulation of a transmitted current. This high-frequency modulation cannot be used for the creation of a slow wave needed for ion acceleration. Therefore, the authors [5] have suggested creating the low-frequency modulation by using the same plasma ions that will be accelerated up to high energies in the second section of a collective accelerator. Ions of plasma are accelerated by the VC field to the area of minimum of its potential. The passed ions will neutralize the space charge of an

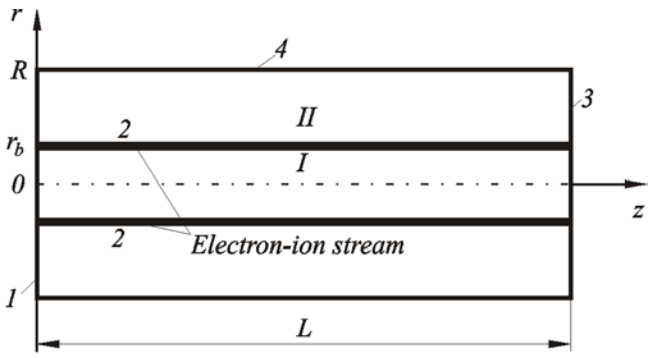

Fig. 1. Annular electron-ion stream in the cylindrical resonator

electron cloud in the VC area, which leads to disappearing VC. The destruction of VC stops the accession of ions to the VC location. Thus, the conditions for the VC formation renew, and the process repeats.

Below, we consider another mechanism of creation of the low-frequency modulation due to ions that are injected in the drift chamber in the same direction, as that of the electron beam. The injected ion-beam current is confined, similarly to that of the electron beam, by the limiting value which is determined by [7]

$$I_{ci} = \frac{Mc^3}{e} \frac{\left(\gamma_i^{2/3} - 1\right)^{3/2}}{2\ln\left(R/r_i\right)}, \tag{2}$$

where M is the ion mass, γ_i is the relativistic factor, and r_i is the radius of an ion beam.

We can conclude from comparison of expressions (1) and (2) that the ion limiting current is much less than the electron current $I_{ci}/I_{ce} \sim \sqrt{m/M}$ even at comparable energies of electron and ion beams. At currents greater than I_{ci} near the input end of the drift chamber, the positive cloud of charges [the virtual anode (VA)] that reflects ions of the ion beam is formed. The frequency of oscillations of VA is much lower than the frequency of oscillations of VC. At the currents of injected ion and electron beams of order of the limiting values, $\omega_i/\omega_e \sim \sqrt{m/M}$ (ω_i is the frequency of oscillations of VA, and ω_e is the frequency of oscillations of VC).

Oscillations of VA will lead to oscillations of an ion current at the input and output of the drift chamber. The temporal dependence of the charge compensating that of an electron beam will lead to the modulation of the electron beam with low frequency. The virtual cathode is a strongly nonlinear formation even in the absence of plasma. For the full description of it, numerical methods are mainly used. Taking into account the dynamics of plasma complicates still further the behavior of VC.

In the present work, the results of numerical simulations of the dynamics of VC in the presence of low-energy ions in the cylindrical resonator are given.

1. Numerical Simulation Algorithm

The algorithm of numerical simulations is based on the particle-in-cell method [11]. Thin annular electron and ion beams are injected in the cylindrical drift chamber of radius R and length L through a metal foil which is transparent for particles. The drift chamber is placed into a strong magnetic field sufficient to consider the motion of particles of a beam as one-dimensional. We assume that the radii of electron and ion beams coincide: $r_e = r_i = r_b$. The specified assumption is not signifiicant for the algorithm of numerical simulations. A generalization to the case of different radii of thin beams can be carried out by the introduction of an additional boundary condition similar to the written one.

The stream (electron and ion beams) divides the drift space into two areas: I: $0 \le r \le r_b$ and II: $r_b \le r \le R$ (see Fig. 1). It allows searching the solution of Maxwell's equations without current sources in each of areas, and the coupling between them will be established through boundary conditions on the stream surface. As there is only the longitudinal component of the beam current density, the longitudinal E_z and radial E_r components of the electric field and the azimuthal component H_φ of the magnetic field will have nonzero values. They are coupled by the system of Maxwell's equations:

$$\frac{\partial E_r}{\partial t} = -c\frac{\partial H_\varphi}{\partial z},$$

$$\frac{\partial E_z}{\partial t} = \frac{c}{r}\frac{\partial}{\partial r}\left(rH_\varphi\right),$$

$$\frac{\partial H_\varphi}{\partial t} = c\left(\frac{\partial E_z}{\partial r} - \frac{\partial E_r}{\partial z}\right). \tag{3}$$

Boundary conditions consist in vanishing the tangential component of the electric field on the metal walls of the resonator and in the reversal of E_r and H_φ at zero at $r = 0$. On the beam surface, the values of E_r, H_φ, and $\partial E_z/\partial r$ have the jumps determined by the surface density of charge and current:

$$E_r^{II} - E_r^I = 4\pi\sigma,$$

$$H_\varphi^{II} - H_\varphi^I = \frac{4\pi}{c} j,$$

$$\frac{\partial E_z^{II}}{\partial r} - \frac{\partial E_z^{I}}{\partial r} = \frac{4\pi}{c^2}\frac{\partial j}{\partial t} + 4\pi\frac{\partial \sigma}{\partial z}, \tag{4}$$

where $\sigma(z,t) = \sigma_e(z,t) + \sigma_i(z,t)$, σ_e and σ_i are the surface charge densities of electrons and ions; $j(z,t) = j_e(z,t) + j_i(z,t)$ is the summary density per unit length of electron and ion currents.

The numerical solution of the system of equations is carried out on the shifted space and time grids. The function E_r is determined at $t^n = n\tau$ (τ is a time step) at the integer grid nodes in longitudinal and transversal coordinates. The function E_z is determined at the same time, but at grid nodes shifted by half a step along the longitudinal and transversal coordinates. The magnetic field H_φ is calculated at half-integer time points at grid nodes shifted relative to the grid of E_r by half a step along the longitudinal coordinate. The radius of an electron beam r_b is supposed to a multiple grid spacing by radius. The field E_z on a beam at $r = r_b$ is calculated through a jump of its derivative and the equations approximating E_z^I and E_z^{II} from the internal nodes of computational regions. The same procedure with the usage of Maxwell's equations allows us to derive $E_r^{I,II}$ and $H_\varphi^{I,II}$ on the beam surface. The expressions for fields approximated in this way on the beam surface at $r = r_b$ contain the surface charge density $\sigma(z,t)$ and linear current density $j(z,t)$ at grid nodes. The surface charge density is calculated by the mechanism of charge weighting according to the particle-in-cell method. The size of particles was selected equal to a grid pitch, which corresponds to the "cloud-in-cell" (CIC) method. Therefore, the weighting of a charge was implemented at two nearest grid nodes. A grid current was determined from the continuity equation.

The equations of motion of macroparticles

$$\frac{dp_k}{dt} = q_k E_z, \quad \frac{dx_k}{dt} = v_k, \tag{5}$$

where v_k is the z-component of a macroparticle velocity, $p_k = m_k v_k \gamma_k$ is the macroparticle momentum, x_k is a coordinate, m_k is the rest mass, q_k is the charge of the k-th macroparticle (macroelectron or macroion), $\gamma_k = \left(1 - v_k^2/c^2\right)^{-1/2}$ is the relativistic factor, were calculated according to the time-centered "overstep" (or "leap-frog") scheme. The force which affects a macroparticle is calculated by a linear interpolation of the electrical field from two grid nodes nearest to the particle.

To control the numerical model accuracy, the energy conservation law was used,

$$W_F(t) + W_P(t) = S(t), \tag{6}$$

where

$$W_F(t) = \frac{1}{8\pi}\int_0^R\int_0^L \left(E_r^2 + E_z^2 + H\varphi^2\right) r\,dr\,dz \tag{7}$$

is the electromagnetic energy in the resonator;

$$W_P(t) = \sum_{\substack{k,\\ 0 \le x_k \le L}} m_k c^2(\gamma_k - 1) \tag{8}$$

is the kinetic energy of macroparticles in the resonator;

$$S(t) = \sum_{k=1}^{N(t)} m_k c^2(\gamma_{0k} - 1) \quad - \\ - \sum_{\substack{k,\\ x_k > L,\ x_k < 0}} m_k c^2(\gamma_{0k} - 1) \tag{9}$$

is the difference between the kinetic energy of all $N(t)$ macroparticles injected in the drift chamber and the energy of macroparticles left the resonator.

2. Numerical Simulation of an Electron-Ion Stream

The above-mentioned algorithm was realized by a complex of programs in language C ++. For testing a numerical code, the parameters of the upgraded version of the experimental installation "Agate" were selected as follows: $R = 2.5$ cm, $r_b = 1.625$ cm, the input beam current $I_b = 4.6$ kA, the energy of beam electrons $eU_b = 280$ keV, and $L = 15$ cm. For such sizes of the drift chamber and parameters of an electron beam space, the charge limiting current is equal to $I_{ce} = 3.8$ kA. For the plasma simulation, low-energy ($eU_i = 28$ keV) hydrogen and nitrogen ions were injected into the system. The ion current ($I_i = 92$ A for hydrogen and $I_i = 25$ A for nitrogen) was selected so that the unperturbed densities of ions and electrons were approximately equal. The radius of an ion stream coincided with that of an electron beam. The limiting current I_{ci} (2) equals $\simeq 3.2$ A for ions of hydrogen and $\simeq 0.87$ A for ions of nitrogen.

At the injection of only an electron beam in the drift chamber, the well-known state with VC was formed inside the drift chamber. The non-stationary process of its formation is finally replaced by a quasistationary one, in which VC parameters periodically oscillate in time. The typical characteristics of such a quasistationary state are shown in Fig. 2. Fig. 2,*a*,*b*,*c* shows instant (at the time $t = 5$ ns) pictures of the electron's phase plane,

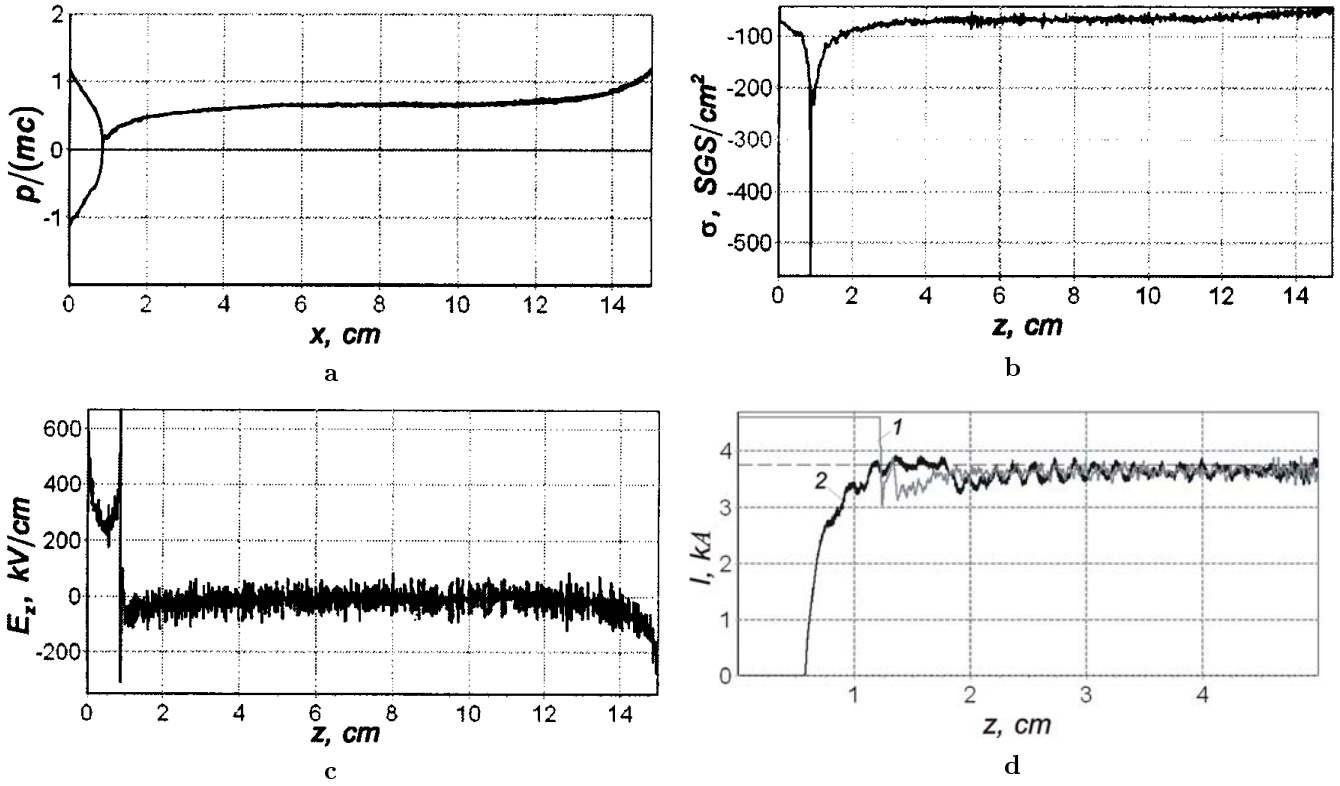

Fig. 2. Characteristics of the virtual cathode in the vacuum cylindrical drift chamber at the time $t = 5$ ns: a phase plane (*a*); longitudinal distributions of surface density of a charge (*b*) and an axial electric field E_z (*c*); time dynamics of the current of an electron beam at the input ($z = 0$, curve *1*) and the output ($z = L$, curve *2*) of the drift chamber (*d*)

and longitudinal distributions of the charge surface density and an axial electric field E_z. In Fig. 2,*d*, the time dynamics of an electron beam current at the drift chamber input ($z = 0$, a curve *1*) and the output ($z = L$, a curve *2*) is depicted. One can see that, at the time $t = 1.19$ ns, the input current sharply decreases. At this time, electrons reflected from VC reach the beginning of the drift chamber, which causes a sharp decreasing of the total current. At a later time, the input current shows time oscillations remaining, on the average, less than the critical value. The output current increases at the beginning, reaches the saturation, and then oscillates in time with the same period, as the input current. The frequency of these oscillations is about ~ 7 GHz.

The dynamics of processes at the joint injection of an electron beam and a stream of hydrogen ions occurred by the following scheme. For the times of order of 1 ns, the electron VC within 1.0 cm apart from the left-hand end of the drift chamber is formed. The main characteristic feature of this stage is a small amount of ions in the system. Therefore, the VC parameters are practically completely determined by electrons (Fig. 3). Nevertheless, the presence of ions results in that the VC position is shifted by 0.2 cm to the right in comparison with the case where the ion flow in the drift chamber is absent. Ions of hydrogen in the longitudinal electric field of VC are accelerated up to energies determined by the VC potential, i.e. up to the energy approximately equal to the energy of initial electrons. Having reached the bottom of the potential well created by VC, ions move without acceleration with approximately constant energy.

At a later time (see Fig. 4), the accumulation of ions in the system results in moving the electron VC deep down the drift chamber. The electric field strength in the VC area decreases, which is accompanied by its partial destruction. This results in increasing the output current. In addition, right at the beginning of the drift chamber, conditions for the appearance of an ion VA are formed. The occurrence of slowed down ions at the beginning of the drift chamber (Fig. 4,*a*) and the positive density of a surface charge (Fig. 4,*b*) testify to it.

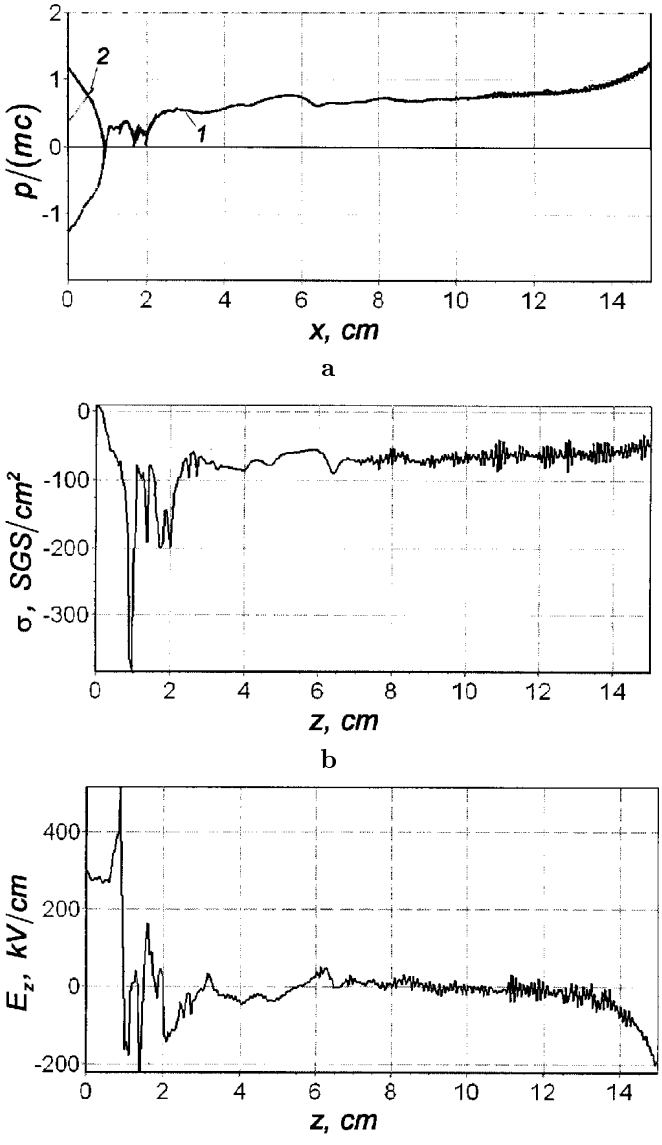

Fig. 3. *a* — a phase plane of electrons (*1*) and ions (*2*); *b* — a surface charge density $\sigma = \sigma_e + \sigma_i$; *c* — a longitudinal electric field at the time $t = 1.54$ ns. In phase planes, the ordinates of the points corresponding to ions are increased by $\sqrt{M/m}$ times

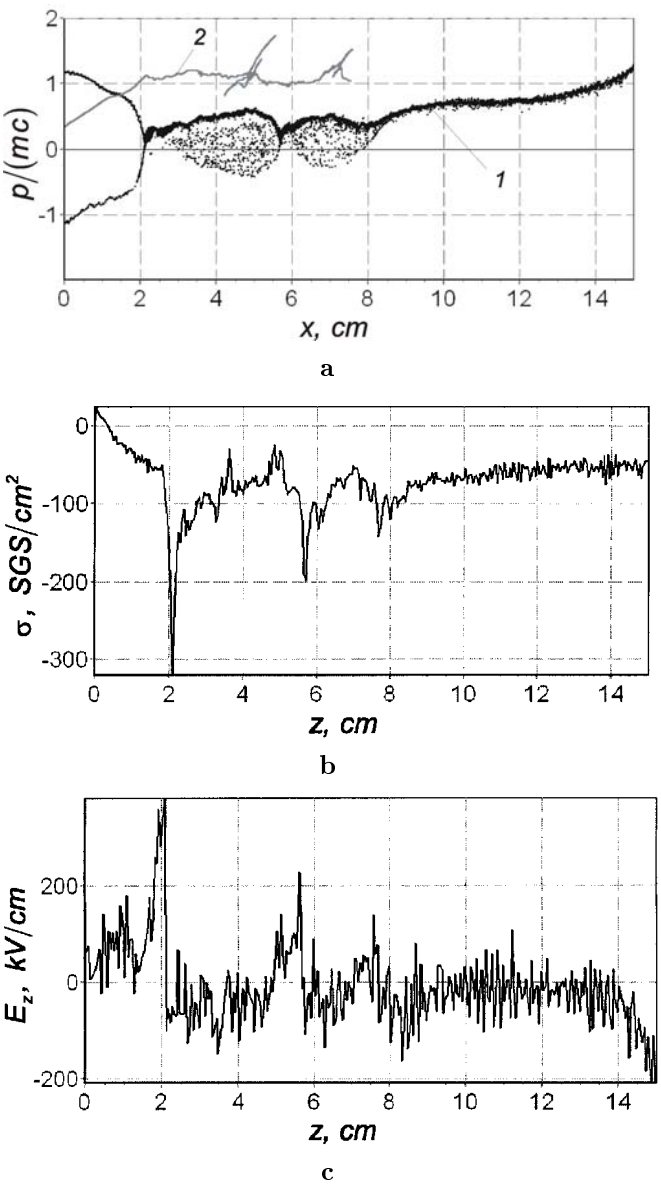

Fig. 4. The same as in Fig. 3 for the time $t = 10.5$ ns

The mentioned factors result in the formation of VA in the system at the time $t = 18$ ns. At the same time, the electron VC practically completely breaks down.

The further interaction of electron and ion streams takes place without formation of VC. Strongly slowed down electrons (see Fig. 4) leave the resonator in the course of time and, being again injected, are slowed down to a much smaller extent, but, at the same time, are strongly thermalized. The typical pattern of such a situation is illustrated in Fig. 5.

The VA pulses in time, periodically disappearing and appearing, which reduces to the occurrence of pulses on the curve of the input current and to the modulation of the output electron current of VC (see Fig. 6). For hydrogen ions, the frequency of pulsations is 300 MHz.

Like that described above, the simulation has been done at the injection of nitrogen ions in the drift chamber. Qualitatively, the pattern of the dynamics of processes repeats. The frequency of pulsations of currents at the input and output of the drift chamber is 100 MHz, i.e. it has decreased approximately in a

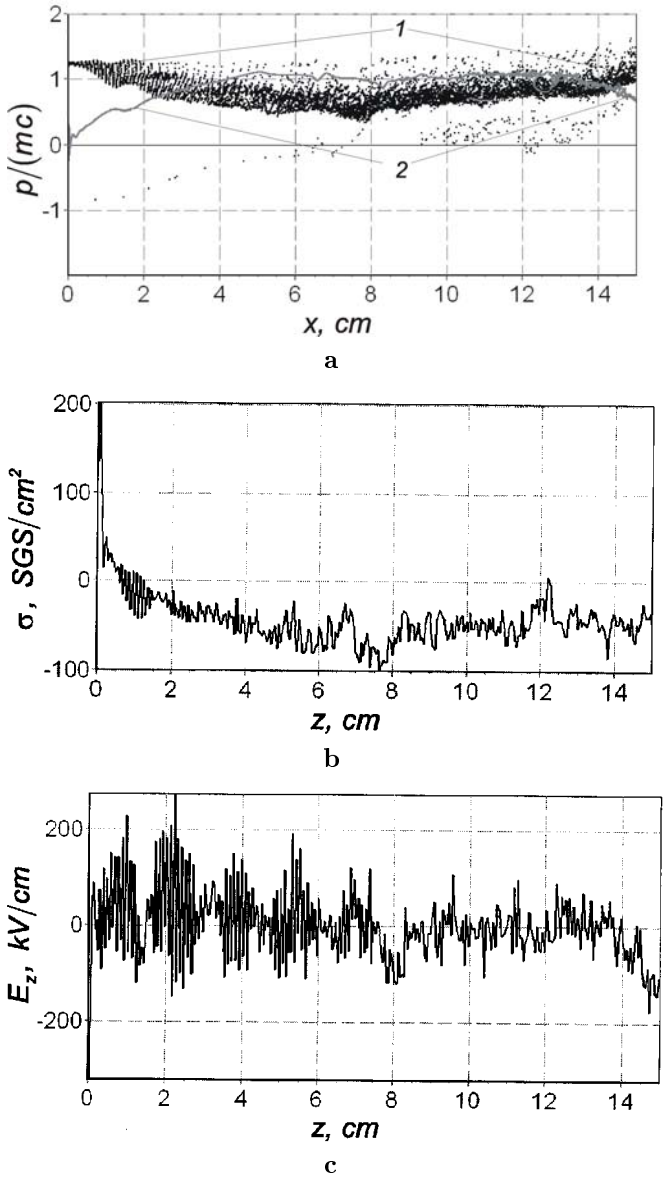

Fig. 5. The same as in Fig. 3 at the time $t = 23.97$ ns

proportion of the square root of the ratio of the masses of ions of nitrogen and hydrogen. As compared to hydrogen, at the injection of nitrogen ions against the background of pulsations of VA, the regime of periodic occurrence of the electron VC is possible as well. This process is much more slow than that mentioned above, because it is connected with the transition time of ions through the drift chamber. The flicker frequency of the electron VC is approximately 5 times lower than the frequency of pulsations of the ion VA.

In Fig. 7,*a*, the power characteristics determined according to expressions (6)—(9), at the injection of an

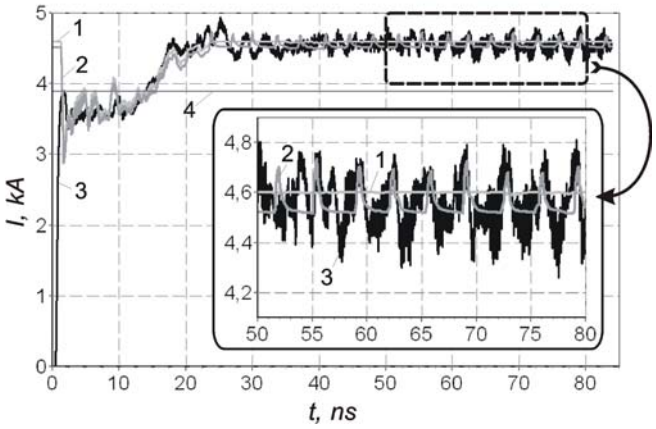

Fig. 6. Time dynamics of the electron (*1*) and total (*2*) currents at the input and the total current at the output (*3*) of the resonator; the direct line (*4*) shows the space charge limiting current of an electron beam in the vacuum drift chamber

electron beam in the resonator are given. We note, first of all, a rather exact performance of the energy conservation law (6) for the calculation times in our algorithm (see Fig. 7,*b*). The error of calculations on the estimated times did not exceed 2.5 %.

In Fig. 8, similar power characteristics at the joint injection of electron and ion streams in the resonator are represented. By the moment of occurrence of the ion VA, the inaccuracy in terms of the conservation energy law (6) made a fraction of percent (Fig. 8, *b*). The maximal error during later instants did not exceed 7 %. As particles are losing their kinetic energy $W_P(t)$, the electromagnetic field energy $W_F(t)$ grows and, at the moment of VC formation, it reaches a local maximum. Without ions at the next times, the energy of particles in the resonator remained approximately stationary, and the electromagnetic field energy grew up still some time to saturation (see Fig. 7,*a*). It's concerned with prolonging the "pumping" of energy in the resonator by newly injected electrons.

At the additional ion injection in the drift chamber, the energy dynamics in the system develops by another way. The energies of particles and electromagnetic field in the resonator after the origin of VC prolong to grow on (see Fig. 8,*a*). This concerns with increasing the transmitted electron current due to the electronic space charge compensation. The growth of particles' energy is prolonged up to the instant of VA origin. At this time, the total and electron currents go out to saturation (Fig. 6), and the number of particles in the resonator

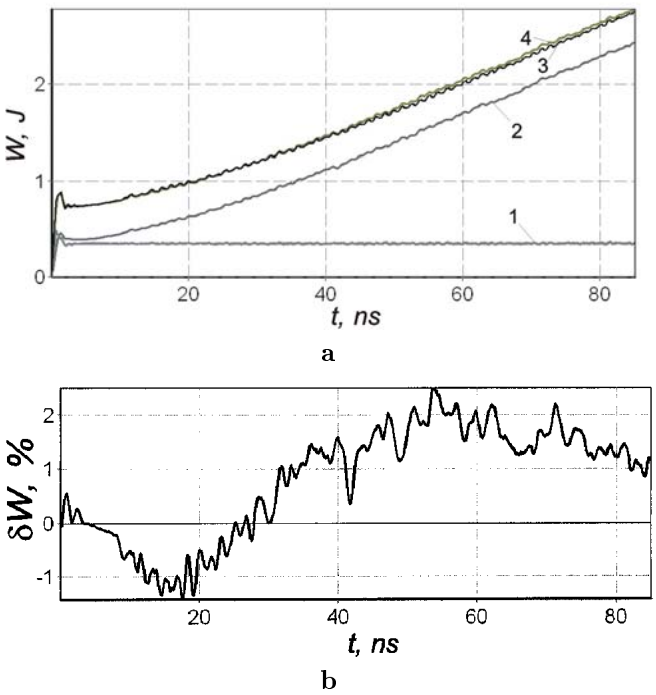

Fig. 7. *a* — power characteristics of VC determined according to expressions (6)—(9), at the injection of an electron beam in the resonator: *1* — $W_P(t)$; *2* — $W_F(t)$; *3* — $W_P(t) + W_F(t)$; *4* is $S(t)$; *b* — a discrepancy from the conservation energy law (6) in a system, $\delta W = (W_F + W_P - S)/(W_F + W_P)$

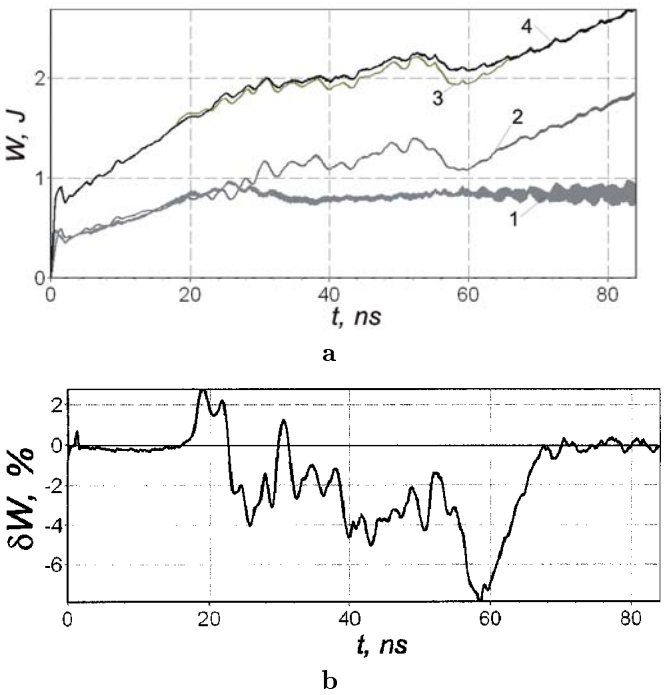

Fig. 8. The same as in Fig. 7, for the joint injection of electron and ion streams in the resonator

remains approximately stationary at a later time. The electromagnetic field energy and the energy loss of particles grow and go out to saturation at $t = 37$ ns.

The further dynamics of the system is determined by the interaction of electron and ion streams. The total and electron currents at the resonator output oscillate around the equilibrium values exceeding the space-charge limiting electron current. The frequency of these oscillations is much lower, and the amplitude is much higher, than those in a case of only the electron beam injection (see, for comparison, Fig. 2,*d* and Fig. 6).

Conclusion

The numerical simulation has shown that the non-stationary dynamics of propagation of a supercritical relativistic electron beam at the injection of a low-energy ion stream develops by the following way. At the initial stage, a VC has been formed in the drift chamber. The parameters of VC are practically wholly determined by an electron beam. Injected ions are accelerated in the potential well of VC and eventually destroy it. The accumulation of the space charge of ions leads to the formation of VA in the drift chamber. The VA periodically pulsates with a low frequency: at the injection of hydrogen ions, this frequency is 300 MHz, and it is 100 MHz for ions of nitrogen. Pulsations of VA lead to changing the output electron current with the same low frequency.

In that way, the investigated mechanism of low-frequency modulation of REB can be used for the creation of a space charge slow wave in the second stage of a collective accelerator of ions where REB is modulated periodically in space.

The given analysis is made under the assumption of a one-dimensional motion of electrons and ions. The condition for a one-dimensional motion of electrons of a relativistic electron beam can be satisfied with imposing an external magnetic field with mild strength. The condition for neglecting the transversal motion of ions during their propagation in the vacuum drift chamber is $H^2 \gg (Mc^2/e)(E_r/R)$, which would need the presence of an external magnetic field with strength of ~ 100 kOe for ions of hydrogen under the considered conditions. But this strong requirement is essentially reduced if we take into account that, at the joint injection of electron

and ion beams, the radial electric fields considerably decrease. In our numerical simulation, we chose the ion current value from the condition of whole charge compensation of an electron beam. It was caused by the other requirement to compensate VC in the ideology of [5]. Fortunately, such a condition considerably reduces the requirements imposed on the external magnetic field strength for maintenance of the equilibrium laminar motion of an ion beam.

The work is supported by the grant of STCU No. 1569.

1. *Lymar A.G., Khizhnyak N.A., Belikov V.V.* // VANT. A Series: Physics of High Energy and a Atomic Nucleus.— 1973.— N 3(5).— P. 78—81.
2. *Tkach Yu.V., Fainberg Ya.B., Lemberg E.A.*//Pis'ma Zh. Eksp.Teor. Fiz.— 1978.— **28**, N 9.— P. 580—584.
3. *Lebedev A.N., Pazin K.N.* // At. Energ.— **41**.— N 4.— P. 244—247.
4. *Ajrapetov K.Sh.* // Pis'ma Zh. Tekhn. Fiz. **12**.— N 15.— P. 935—938.
5. *Balakirev V.A., Gorban A.M., Magda I.I. et al.* // Fiz. Plazmy.— 1997.— **23**, N 4.— P. 350—354.
6. *Bogdankevich A.S., Rukhadze A.A.*// Uspekhi Fiz. Nauk.— 1971.— **103**, N 4.— P. 609—640.
7. *Miller R.B.* An Introduction to the Physics of Intense Charged Particle Beams.—New York: Plenum Press, 1982.
8. *Kwan J.T.* // Phys. Fluids.— 1989.— **27**, N 1.— P. 228—232.
9. *Alterkop B.A., Sokulin Yu.A., Tarakanov V.P.* //Fiz. Plazmy.— 1989.— **15**, N 8.— P. 974—980.
10. *Alterkop B.A., Rukhadze A.A., Sokulin Yu.A., Tarakanov V.P*// Zh. Tekhn. Eiz. — 1991.— **61**, N 9.— P. 115—123.
11. *Berezin Yu.A., Vshyvkov V.A.* Method of Particles in Dynamics of Rarefied Plasma. — Novosibirsk: Nauka, 1980 (in Russian).

Received 17.06.03

ДО ПИТАННЯ ПРО МЕХАНІЗМ НЧ-МОДУЛЯЦІЇ ПОТУЖНОСТРУМОВОГО РЕЛЯТИВІСТСЬКОГО ЕЛЕКТРОННОГО ПУЧКА

П.І. Марков, І.М. Онищенко, Г. В. Сотніков

Р е з ю м е

Наведено результати досліджень транспортування релятивістського електронного пучка зі струмом, більшим за критичний, в циліндричній камері дрейфу в присутності іонного потоку. Теоретичний аналіз динаміки електрон-іонного утворення грунтується на методі великих частинок (PIC). Показано, що при спільній інжекції надкритичного електронного пучка і низько енергетичного слабострумового іонного пучка в камері дрейфу, поряд з електронним віртуальним катодом може утворитися віртуальний анод. Віртуальний анод періодично пульсує. Чисельні розрахунки, проведені для іонів водню й азоту, показали, що відношення частот пульсацій обернено пропорційне відношенню мас іонів. Коливання віртуального анода приводять до модуляції в часі з тією ж частотою електронного й іонного струмів на виході дрейфової камери.